COMPARATIVE STABILITY ANALYSIS OF D23N MUTATED Aβ

ERIK J. ALRED, EMILY G. SCHEELE, WORKALEMAHU M. BERHANU, AND ULRICH H. E. HANSMANN

Dept. of Chemistry & Biochemistry, University of Oklahoma
Norman, OK 73019, USA

Abstract: Amyloid β (Aβ) is the subject of numerous studies due to its link to the devastating Alzheimer's disease and it exists in a parallel structure in fibril aggregate. The Iowa mutant (D$_{23}$N) Aβ posses a unique antiparallel fibril aggregate structure and can also form parallel structure. This structural difference, coupled with the fact that occurrence of the Iowa mutant is correlated with early onset Alzheimer's, suggests to use these peptides as candidates for computational studies of the structural determinants of the toxicity of Alzheimer's disease. In order to compare the two observed Aβ structural motifs, we designed a computational study to probe the factors that affect the stability of parallel and antiparallel aggregates. Since the structural changes may occur on a timescale beyond that sampled in traditional molecular dynamics (MD), we employed a techniques of scaling the mass to reduce the solution's viscosity and compared the results to regular molecular dynamics. The knowledge gained from this study could provide insight into the mechanism of selection for antiparallel and parallel two fold structures.

Keywords: Iowa mutant, Aβ, structural polymorphism, molecular dynamics, parallel and antiparallel β sheets

1. Introduction

Amyloid plaques are associated with the occurrence of Alzheimer's disease [1] as one of its markers is the presence of amyloid fibrils in patients brains [2]. This aggregation is aided by peptide strands establishing a system of steric-zipper like hydrophobic forces and van der Waals interactions as well as hydrogen bonding interactions [3]. Amyloid aggregates have been observed forming fibrils of differing morphologies due to differences in contact and packing of the peptide residues [4, 5]. These variations in aggregate structure lead to a difference in both the cytotoxicity and nucleation rate [6–8]. One example is the pathological changes between wild type Aβ and the D$_{23}$N Iowa mutant

of Aβ, with the Iowa mutant possessing a much higher neurotoxicity [9]. This is correlated with structural difference between wild type Aβ, which is observed only in parallel β sheets [10], and Iowa mutant Aβ, which can be observed in both parallel and antiparallel β sheets [11]. The presence of this structure questions the long-standing assumption that amyloid fibrils are constructed of parallel β sheet [12]. Since there are also data suggesting that wild type aggregates could contain also antiparallel peptides [13] it seems possible that the higher cytotoxicity in the Iowa mutant [9] is related to the higher proportion of antiparallel aggregates. As suggested previously, the stability of these structures is partially related hydrophobic packing of residues. The temperature dependence of hydrophobic interactions means that the stability of the structure will be affected by the artificial dynamics enacted in replica exchange MD and generalized ensemble sampling [14–16]. Thus, we tested an alternative approach to enhance sampling efficiency, namely to reduce viscosity through mass scaling as suggested in previous studies [17, 18]. Using our scaled systems we probed the stability of the antiparallel and parallel systems for the wild type and Iowa mutant amino acid sequences.

2. Experimental Methods

Molecular dynamic simulations were performed on hairpin loop fold decamers constructed from solid state NMR structural data of the aggregates (PDB codes 2LNQ and 2LMO). The antiparallel model was constructed with the assumption that the wild type's antiparallel structure would be similar to the experimentally observed one of the $D_{23}N$. Therefore, residue 23 of the characterized structure for antiparallel Iowa mutant (2LNQ) was replaced with aspartic acid (D) to create a wild type Aβ antiparallel decamer. A similar method was employed to create a parallel Iowa mutant structure from the wild type 2LMO, with the residue 23 being replaced by asparagine (N). The parallel system's residues 10–14 were then truncated from the original 10–40 peptide chain to a chain of residues 15–40, that of the antiparallel model. The antiparallel model required construction of a two fold system from the experimentally characterized single fold system by positioning two pentamer systems in a distance of 9–10 Å as observed in previous studies [1]. The resulting 4 systems were then simulated using molecular dynamics with the CHARMM27 force field and CMAP corrections [19–21] as implemented in GROMACS version 4.6.2 [22]. The explicit solvent TIP3P [21, 23] was selected for the all atom solution to generate the solvent box. The decamer was centered in a cubic box of a distance at least 12 Å from the protein [24]. The temperature was set to normal body temperature of 310 K. After minimization and equilibration, three 300 ns trajectories were run for both half and full mass variants of the all systems, making a total of 24 trajectories. Overlays of the initial and final structures are shown in Figure 1.
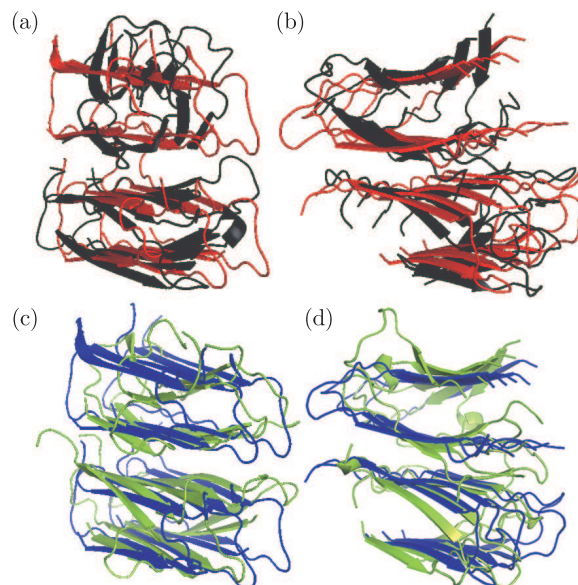
Figure 1. This figure compares the scaled mass structures of the initial and final for Iowa mutant (red and black respectively) and wild type (blue and yellow respectively); **(a)** shows the antiparallel Iowa mutant, **(b)** shows the parallel Iowa mutant, **(c)** shows the antiparallel wild type, and **(d)** shows the parallel wild type

3. Results: RMSD/RMSF

Comparison of the average root mean standard deviation (RMSD) of the three trajectories over the first 200 ns shows gains in mass scaling. The antiparallel Iowa mutant (Figure 2 a) shows that both the full mass and half mass system reach a RMSD from the original structure of 6 Å. However, mass scaled system, indicated by the blue line, on average reaches this RMSD value after 7 ns, compared to the full mass control's 104 ns indicates an overall efficiency increase of 15 fold. The other systems show similar increases, though the two RMSD charts never reach parity (Figure 2 b–d). Differences between the half mass and full mass root mean standard fluctuations (ΔRMSF) for the simulations (Figure 2 e–h) shows little behavioral difference with scaled masses. This suggests similar behavior between the systems, though further studies are needed to investigate other changes. Comparison of RMSD values between parallel and antiparallel structures of the same sequence shows an overall decrease of 1 Å indicating the preference of the parallel structure. This is likely due the decreased motion of residues in the second β sheet (residues 29–37). Comparison of the RMSD/ΔRMSF values between Iowa mutant and wild type shows no discernable difference.

4. Results: Hydrogen Bonding of residue 23

Observations of the hydrogen bonding nature of residue 23 suggest that the Iowa mutant has increased potential to form inter-protein hydrogen bonds. This is shown by (Figure 3 a–d) in which the Iowa mutants shown in parts (a) and (c)
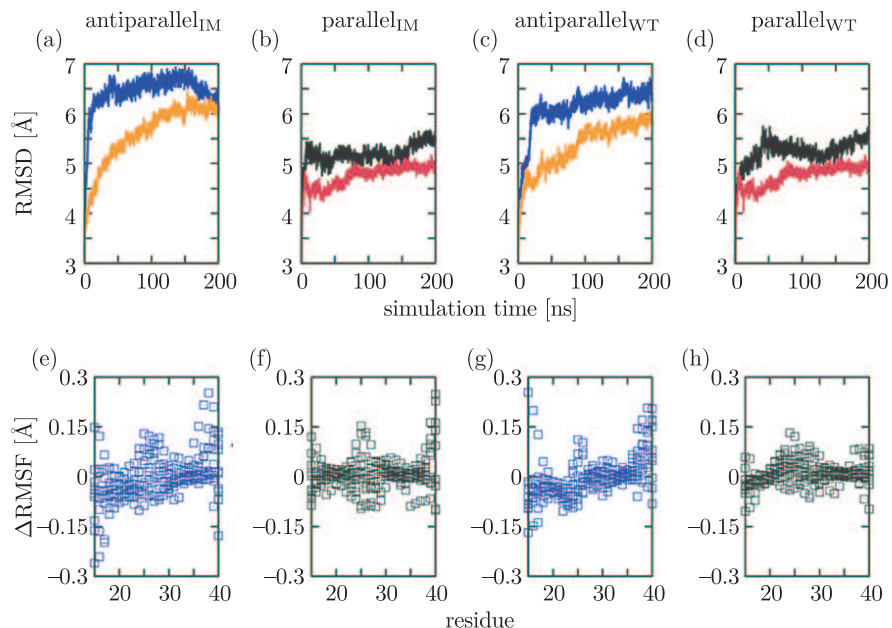
Figure 2. Shows the RMSD for the first 200 ns and ΔRMSF of the simulations for half and full mass systems. ΔRMSF is defined as the difference between the half mass run and the full mass run; **(a/e)** show the RMSD/ΔRMSF of the antiparallel Iowa mutant for full mass (orange) and half mass (blue); **(b/f)** show the RMSD/ΔRMSF of the parallel Iowa mutant for full mass (red) and half mass (black); **(c/g)** show the RMSD/ΔRMSF of the antiparallel wild type for full mass (orange) and half mass (blue); **(d/h)** show the RMSD/ΔRMSF of the parallel wild type for full mass (red) and half mass (black)

have on average 12 protein-protein hydrogen bonds per system compared to the wild types 5. Note that since there were 10 peptide chains measured, that several arginine must have performed multiple hydrogen bonding interactions. Conversely, only half of the 10 aspartic acid residues are forming hydrogen bonds at any given point in time. This behavior is shared between parallel and antiparallel structures, providing a possible explanation to the increased stability of Iowa mutant antiparallel aggregates. Note that the protein solvent hydrogen bonding is higher for the wild type than Iowa mutant at residue 23 (Figure 3 e–h).

5. Results: DSSP calculations

Results of secondary structure analysis was performed for the first and last 100 ns of the simulation. The results are compiled in Figure 4. As shown, there is approximate difference of 5% beta sheet content between antiparallel and parallel structures of the same sequence, with antiparallel possessing more beta sheet character. This is likely due to the truncations of residues 10–14 in parallel systems, which removed residues normally present in β sheet configuration. However, these results indicate that β do not play the sole role in the observed increased stability between the parallel and antiparallel systems.
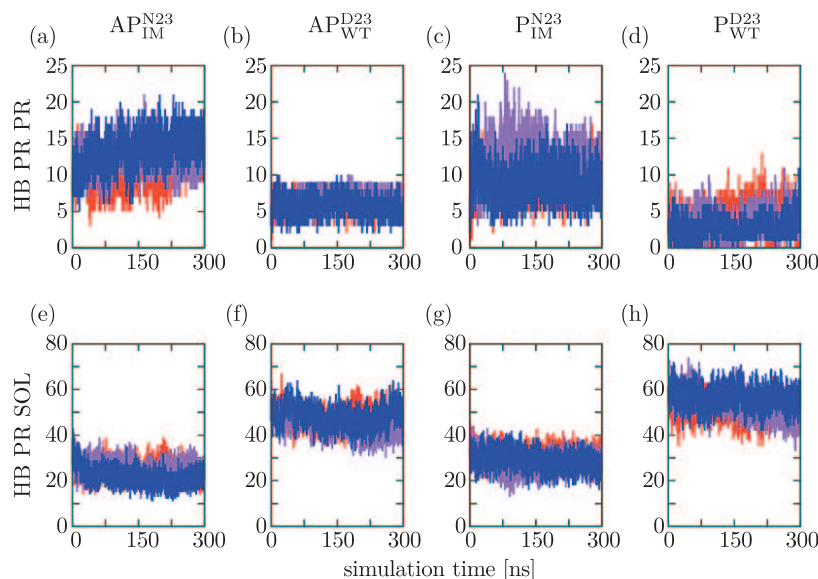
Figure 3. Shows the number of hydrogen bonds formed by residue 23; **(a/e)** show the protein protein/protein solvent hydrogen bonding for residue 23 of antiparallel Iowa mutant; **(b/f)** show the protein protein/protein solvent hydrogen bonding for residue 23 of antiparallel wild type; **(c/g)** show protein protein/protein solvent hydrogen bonding for residue 23 of parallel Iowa mutant; **(d/h)** shows protein protein/protein solvent hydrogen bonding for residue 23 of parallel wild type
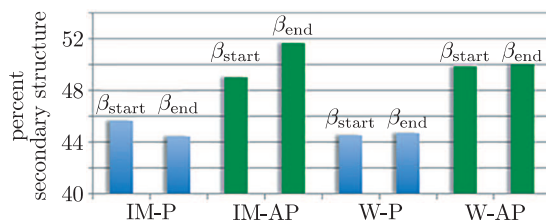
Figure 4. Shows the percentage secondary structure of β sheets; these are divided between the first and last 100 ns of simulation time indicated by β_{start} and β_{end} respectively; the following abbreviations are used on the x axis in order of appearance: Iowa mutant parallel: IM-P; Iowa mutant antiparallel: IM-AP; wild type parallel: W-P; wild type antiparallel: W-AP

6. Conclusion

Based on the results, we can conclude that the mass scaling has a significant effect on the sampling of the observed amyloid MD simulations. Furthermore, we can infer that the hydrogen bonding of the mutated residue 23 plays a large role in the stability of both parallel and antiparallel structures, with an observed increase in protein-to-protein hydrogen bonds for asparagine relative to aspartic acid. Finally, the secondary structure content is not a major factor in the increased parallel stability, as decreasing the beta sheet content did not cause the structure to become less stable than the antiparallel conformation. These results are preliminary and will be expanded upon in future works.

Acknowledgements

References

[1] Eisenberg D and Jucker M 2012 *Cell* **148** (6) 1188

[2] Ahmed M, Davis J, Aucoin D, Sato T, Ahuja S, Aimoto S, Elliott J I, Van Nostrand W E and Smith S O 2010 *Nat. Struct. Mol. Biol.* **17** (5) 561

[3] Sawaya M R, Sambashivan S, Nelson R, Ivanova M I, Sievers S A, Apostol M I, Thompson M J, Balbirnie M, Wiltzius J J W, McFarlane H T, Madsen A O, Riekel C and Eisenberg D 2007 *Nature* **447** (7143) 453

[4] Petkova A T, Leapman R D, Guo Z H, Yau W M, Mattson M P and Tycko R 2005 *Science* **307** (5707) 262

[5] Fitzpatrick A W P, Debelouchina G T, Bayro M J, Clare D K, Caporini M A, Bajaj V S, Jaroniec C P, Wang L C, Ladizhansky V, Muller S A, MacPhee C E, Waudby C A, Mott H R, Simone A D, Knowles T P J, Saibil H R, Vendruscolo M, Orlova E V, Griffin R G and C M Dobson 2013 *Proc. Natl. Acad. Sci. U.S.A.* **110** (14) 5468

[6] Smaoui M R, Poitevin F, Delarue M, Koehl P, Orland H and Waldispuhl J 2013 *Biophys. J.* **104** (3) 683

[7] Miller Y, Ma B Y and Nussinov R 2009 *Biophys. J.* **97** (4) 1168

[8] Berhanu W M and Hansmann U H E 2012 *PLoS One* **7** (7) ???

[9] Murakami K, Irie K, Morimoto A, Ohigashi H, Shindo M, Nagao M, Shimizu T and Shirasawa T 2003 *J. Biol. Chem.* **278** (46) 46179

[10] Petkova A T, Yau W M and Tycko R 2006 *Biochemistry* **45** (2) 498

[11] Tycko R, Sciarretta K L, Orgel J and Meredith S C 2009 *Biochemistry* **48** (26) 6072

[12] Tycko R 2011 *Annu. Rev. Phys. Chem.* **62** 279

[13] Schmechel A, Zentgraf H, Scheuermann S, Fritz G, Pipkorn R D, Reed J, Beyreuther K, Bayer T A and Multhaup G 2003 *J. Biol. Chem.* **278** (37) 35317

[14] Hansmann U H E and Okamoto Y 1993 *J. Comp. Chem.* **14** 1333

[15] Hansmann U H E 1997 *Chem. Phys. Lett.* **281** 140

[16] Sugita Y and Okamoto Y 1999 *Chem. Phys. Lett.* **314** (1–2) 141

[17] Lin I C and Tuckerman M E 2010 *J. Phys. Chem. B* **114** (48) 15935

[18] Wright L B and Walsh T R 2013 *Physical Chemistry Chemical Physics* **15** (13) 4715

[19] Foloppe N and MacKerell A D 2000 *J. Comput. Chem.* **21** (2) 86

[20] MacKerell A D, Bashford D, Bellott M, Dunbrack R L, Evanseck J D, Field M J, Fischer S, Gao J, Guo H, Ha S, McCarthy D J, Kuchnir L, Kuczera K, Lau F T K, Mattos C, Michnick S, Ngo T, Nguyen D T, Prodhom B, Reiher W E, Roux B, Schlenkrich M, Smith J C, Stote R, Straub J, Watanabe M, Wiorkiewicz-Kuczera J, Yin D and Karplus M 1998 *J. Phys. Chem. B* **102** (18) 3586

[21] Zachariae U, Schneider R, Briones R, Gattin Z, Demers J P, Giller K, Maier E, Zweckstetter M, Griesinger C, Becker S, Benz R, Groot B L de and Lange A 2012 *Structure* **20** (9) 1540

[22] Pronk S, Pall S, Schulz R, Larsson P, Bjelkmar P, Apostolov R, Shirts M R, Smith J C, Kasson P M, Spoel D van der, Hess B and Lindahl E 2013 *Structural bioinformatics* **29** (7) 845

[23] Kutzner C, Grubmuller H, Groot B L de and Zachariae U 2011 *Biophys. J.* **101** (4) 809

[24] Buchanan L E, Carr J K, Fluitt A M, Hoganson A J, Moran S D, Pablo J J, Skinner J L and Zanni M T 2014 *PNAS* **111** (16) 5796